Scientific Research Publishing

International Journal of Geosciences, 2023, 14, 251-269
https://www.scirp.org/journal/ijg
ISSN Online: 2156-8367
ISSN Print: 2156-8359

Lithostratigraphic and Geochemical Characterization of Tobene Phosphate Deposits: A Case Study of Tobene South 1

Ndeye Khady Ndiaye[1], Mouhamadoul Bachir Diouf[2]

[1]Pan African University for Life and Earth Science Institute, University of Ibadan, Ibadan, Nigeria
[2]Département de Géologie, Faculté des Sciences et Techniques, Université Cheikh Anta Diop, Dakar, Senegal
Email: ndiayemaman@live.fr

How to cite this paper: Ndiaye, N.K. and Diouf, M.B. (2023) Lithostratigraphic and Geochemical Characterization of Tobene Phosphate Deposits: A Case Study of Tobene South 1. *International Journal of Geosciences*, **14**, 251-269.
https://doi.org/10.4236/ijg.2023.142013

Received: October 27, 2022
Accepted: February 25, 2023
Published: February 28, 2023

Abstract

Tobene is the third exploitation panel of the Taiba Phosphate deposits. It is divided into five sectors and its exploitation started in 2003 after the closure of the Ndomor and Keur Mor Fall panels. The Taiba phosphate deposit has been the object of several studies based on lithology, biostratigraphy, geochemistry, and petrography; however, few investigations on the variation in thickness of the phosphate layer within the Tobène sector have been conducted. This study seeks to analyze the lithostratigraphic and geochemical characteristics of the phosphate layer in the Tobène South1. Results from the lithostratigraphic study show from top to bottom the following succession: the sandy overburden, the sandstone formation, the Silico-feralitic formation, the variegated roof clays, the Taiba formation (homogeneous ore and heterogeneous ore), and the foliated attapulgite of the wall. Geochemical analysis reveals an unequal distribution of major oxides (P_2O_5, CaO, Fe_2O_3, Al_2O_3, and SiO_2). The area is dominated by P_2O_5 concentrations between 20% and 32%, the K parameter (=CaO/P_2O_5) has an average of 1.36. The iron associated with aluminum (feral) is present in the southern part and on the contours of the sector; the dominant silica concentration is 20%. Correlations established between the major oxides show a strong relationship with p-values << 0.05, nevertheless there is proportionality in the evolutions between the chemical variables CaO and P_2O_5, on the other hand, an opposite evolution between P_2O_5 and the two chemical parameters silica (SiO_2) and feral.

Keywords

Tobene, Taiba, Keur Mor Fall, Ndomor, Sandy Recovery, Silico-feralitic

1. Introduction

The Senegalo-Mauritanian Basin results from the separation of Africa and North America during the Jurassic. The basin lies between 10˚50', 22˚50'N and 17˚30', 13˚30'W [1]. It is the largest (340,000-km^2) passive margin basin on the African Atlantic coast. It extends over 1400 km between Cape Barbas (Mauritania) and Cape Roxo (Guinea Bissau), through Senegal and the Gambia. Its maximum width is 550 km at the latitude of Dakar and it covers 3/4 of Senegal's surface area [2]. The basin is limited to the North by the metamorphosed and granitized Precambrian basement of the Réguibat ridge, to the East by the Pan-African and Hercynian chain of the Mauritanides, to the South by the Paleozoic basin of Bové (Guinea Bissau) and to the West, it is widely open to the Atlantic Ocean (Figure 1).

Supported by the West African Craton, the coastal basin accumulates a powerful sedimentary series, mainly of marine origin, that begins in the Triassic-Lias and ends in the Miocene [3]. The geological history of the MSGBC basin is complex and can be divided into pre-rift (Upper Proterozoic-Paleozoic), syn-rift (Permian-Triassic), and post-rift (Jurassic-Actual) phases. Sediments deposited between Precambrian and Devonian are mainly continental detrital rocks and constitute the pre-rifting phase [4]. During the syn-rift, Triassic

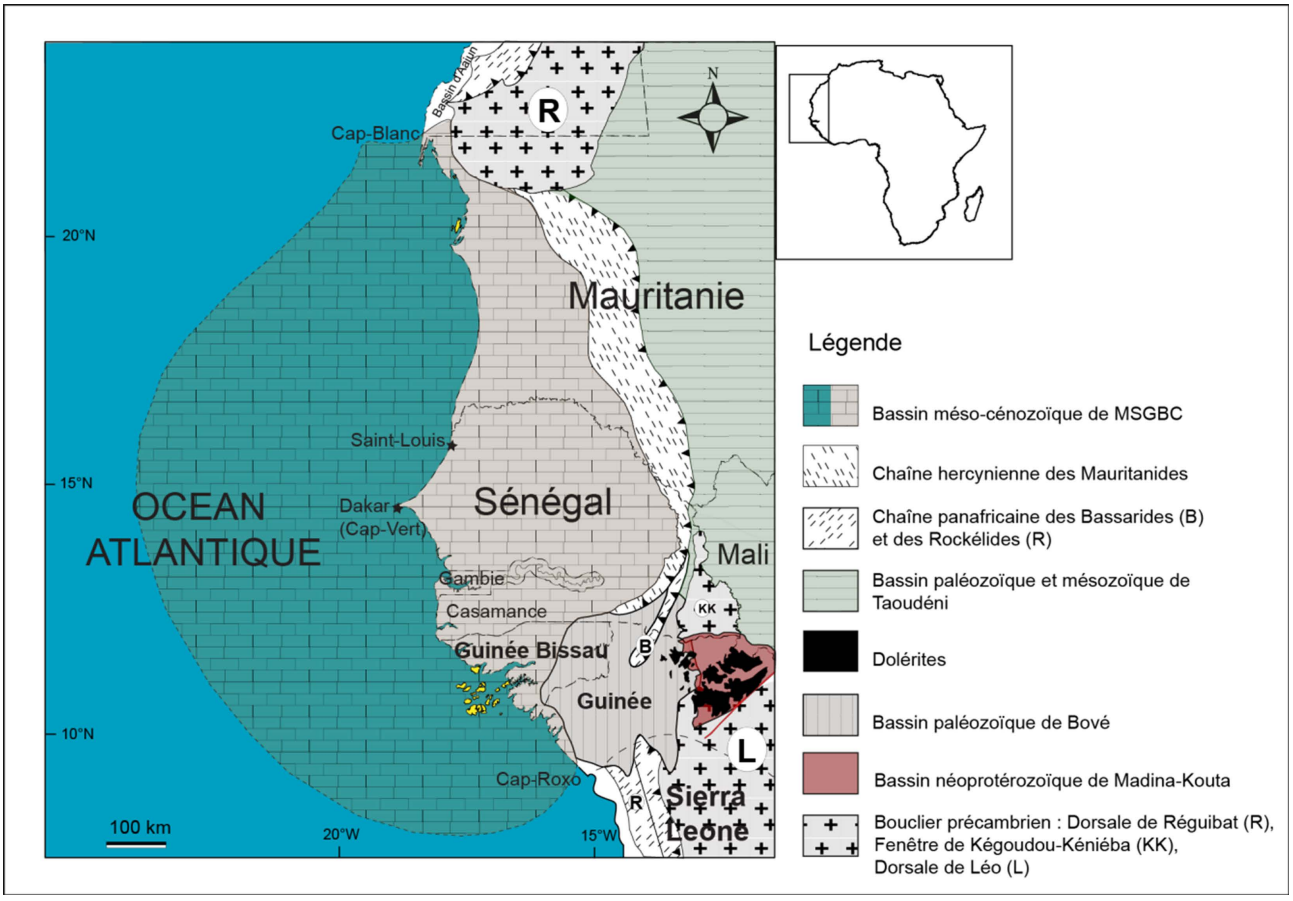

Figure 1. Geological setting of the MSGBC Basin (Ndiaye *et al.*, 2016).

evaporites and Jurassic volcanic intrusion from the Central Atlantic Magmatic Province constituted the main deposit, while a thick Mesozoic-Cenozoic sedimentary cover characterized the post-rift phase [5]. The basin has a simple overall structure, the Mesozoic and Cenozoic deposits form a vast monocline with a slight dip toward the West. Geophysical and well data show the accentuation of the basement dip from Kolobane highlighting two structural domains separated by a flexural zone (Figure 2).

- The Eastern domain, located East of the meridian 15˚30'W has a sedimentary filling of Late Cretaceous and Cenozoic ages. Slight thick sediments (<1000 m) overlie a tilted basement.
- The flexure zone between 15˚30'W and 16˚30'W is characterized by the progressive dip of the basement towards the West. The thickness of the sedimentary deposits increases towards the West to exceed 4200 m at Diourbel.
- The Western distal part of the MSGBC basin is characterized by higher subsidence rates, this domain is located to the west of a "hinge zone" or "rift onset" that trends North-South separating a more stable domain to the East. Several basement lineaments, generally trending East-West, can be mapped and linked to fracture zones offshore.

The stratigraphy within the basin is strongly dominated during Middle Eocene in Thies region by Lam-Lam marl and attapulgite clay known as Lam-Lam Formation; Taiba Formation that is made of limestones and phosphate marls with Nummulites and large flints, variegated clays and flints with "daucines" [3]. The phosphates of Taiba are one of the four areas of calcium phosphate mineralization of the MSGB basin, which has been under exploitation since 1960 [2].

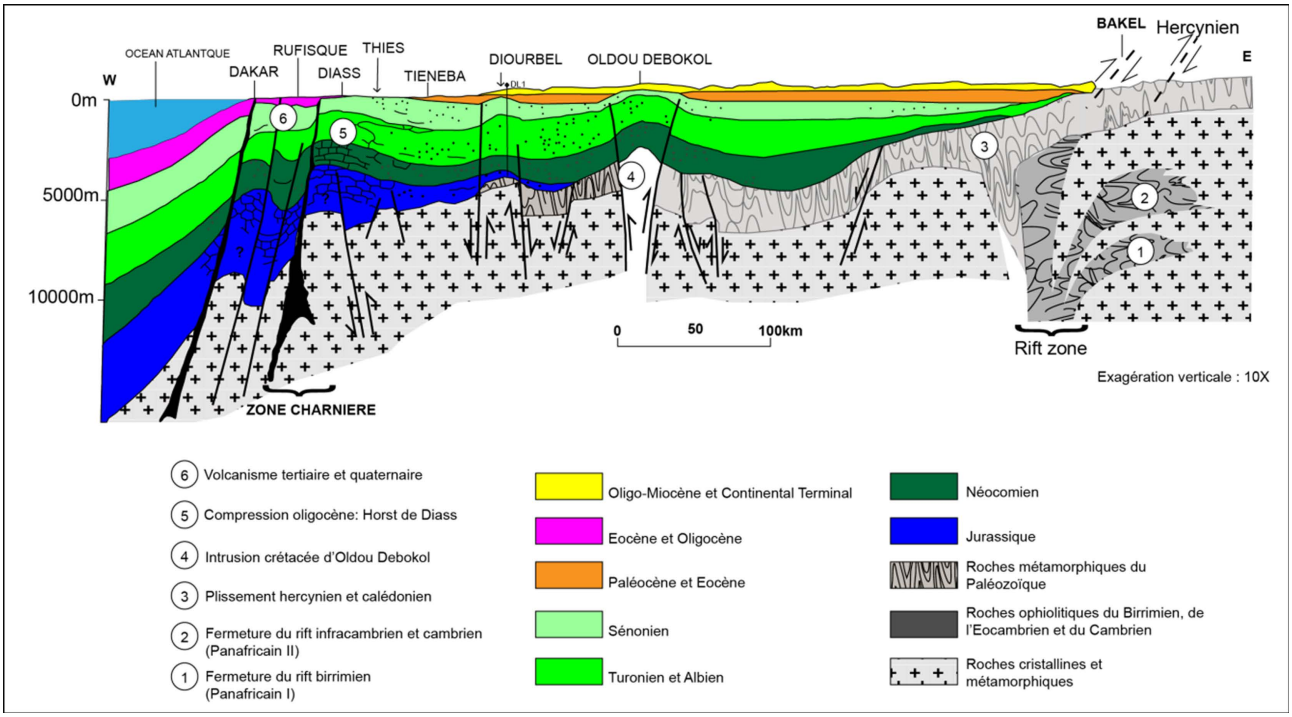

Figure 2. Dakar Bakel cross section in the MSGBC (Ndiaye *et al.*, 2012).

The Taïba deposit is one of the largest phosphate reserves in Senegal, with an estimated tonnage of 63 million marketable tons at 79 BPL over an area of 3000 hectares [6]. It is divided into three sectors: NDOMOR DIOP operated from 1960 to 1980, KEURMORFALL from 1980 to 2003, and TOBENE in operation since 2003. Tobene sector, which hosts our study area, has an estimated reservoir of 50 Mt of phosphate at P_2O_5 27.34% in a single layer of 5.20 m thickness. The Taïba mine exploits a phosphate layer of sedimentary origin caught between a roof and a clayey wall. The aim of this paper is to conduct lithostratigraphic and geochemical characterization of the phosphate layers in Tobène South1 Sector.

2. Geological Context of the Tobène Deposit

Tobene South 1 is part of the Tobene South Centre sector located in the third panel of the Taiba phosphate deposit. The latter lies between 15˚-15˚10' latitude and 16˚45'-17˚ longitude located at North West of the N'Diass dome on which it clings [7]. Tobene and the first two panels of the Taïba deposit belong to the

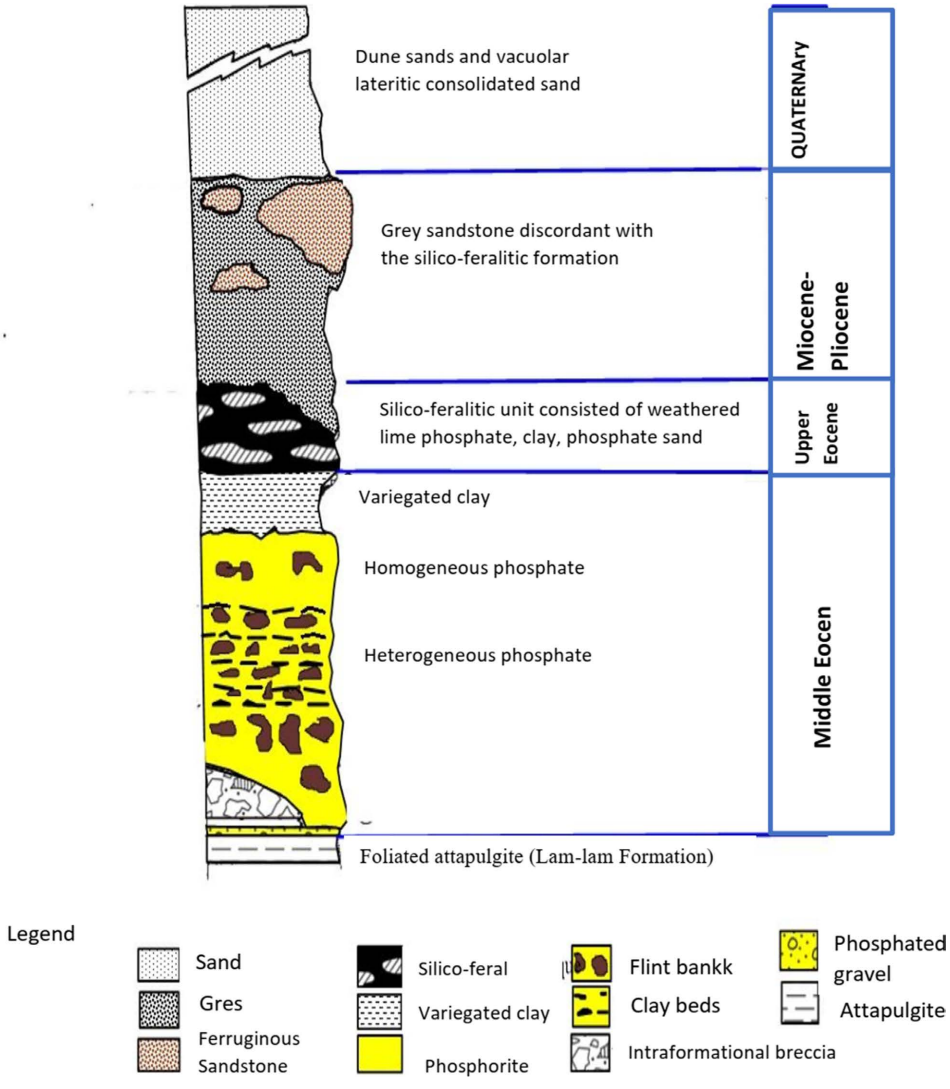

Figure 3. Synthetic log of Tobene deposit modified after (Samb, 1993).

Senegalo-Mauritanian basin, which formed at the culmination of a Permian to Triassic rift system that developed over an extensive Paleozoic basin during the breakup of North America, Africa, and South America [8]. The proposed synthetic log of the deposit has been subject to many revisions. The lithostratigraphic study conducted by [9] in Tobene, has defined the following stratigraphic succession (**Figure 3**):

Lutetian Lam-lam formation constitutes the wall of the deposit; at Tobène, this formation corresponds to finely laminated clays type attapulgite. Lateral variations from clay to limestone facies are frequent within the Tobène sector. On the western margin of the basin, the Lam-Lam Formation is made of marly-carbonate series, phosphatized, 20 meters thick. These deposits are characteristic of a platform environment, rich in diversified macro- and microfauna (mollusks, echinids, and red algae) [3]. The studies conducted by [10], which allowed dating the Lam-Lam formation, reveal that the latter has delivered a fauna rich in planktonic foraminifera (Globorotalia collactea, G. bolivariana, G. pentacamerata, and Hantkenina sp.) typical of the biozonation P10 characteristic of Lutetian.

The Taiba phosphate group:

The first stratigraphic division study was made by [11], who subdivided the Middle Eocene into two parts and distinguished an "upper Lutetian" characterized by the presence of Nummulites (very frequent in the Taiba phosphate deposit). The last revisions of the series [12] have recognized the upper part of the Middle Eocene above the Lam-Lam Marls. They gathered these facies under the stratigraphic subdivision of Taiba Phosphate Group divided into a phosphate Formation with large nodular flints rich in Nummulites gizehensis, overlain by a second formation with platelet flints with daucines and variegated clays. These two formations represent the Taiba Formation of Bartonian Ages with thicknesses up to 12 m. Above the Taiba Formation, the variegated clays of various colors, 2 to 3 m thick, constitute the roof of the phosphate deposit. The Silico-feralitic formation which overlays the roof of the ore corresponds to weathered lime phosphate alternating with levels of highly oxidized clay-phosphate sand towards the top. The thickness of the Silico-feralitic formation varies between 0 to 5 m. It contains intercalations of clay beds.

The sandstone formation is composed of grey clayey sandstone discordant with the Silico-feralitic formation. It is very ferruginous and can appear in the form of armour.

The dune sands (20 to 30 m) consist of irregular sandy banks, consolidated, indurated, and vacuolar laterites of the Quaternary age.

3. Material and Methods

The study was carried out on 117 boreholes. For confidentiality reasons, each borehole was assigned to new projection coordinates x and y arbitrarily defined and plotted in an orthogonal reference frame using Surfer 11 software. Four correlation sections (East-West direction) have been established to estimate var-

iation in the thickness of the phosphate layers within the sector and the litho-stratigraphic correlation was possible thanks to STRATER 4 Software. Figure 4 shows the map of the different boreholes and the correlation sections studied in the sector. The lithological description of the cores was macroscopic using a loop, water, and hydrochloric acid. Geochemical characterization is carried out on particles sized between 25 and 25,000 micrometers at the ICS laboratory. The repartition of major elements within the sector is studied using the isocontent map realized in surfer 11. Correlation between major elements as well as their relationship was possible by interpreting Pearson's product-moment correlation using the statistical software R.

Lithostratigraphic correlations were performed by linking identical facies in each borehole laterally. Geochemical analysis concerns the major elements which are P_2O_5, CaO, SiO_2, Fe_2O_3, and Al_2O_3, and the percentage of each of these major elements is determined following standard methods.

P_2O_5 determination

Determination of the percentage of P_2O_5 consists of nitric oxidation and incineration, the phosphate ore is then colorimetrically dosed with the hydrochloric acid solution of the ashes thanks to the yellow coloration it gives with the

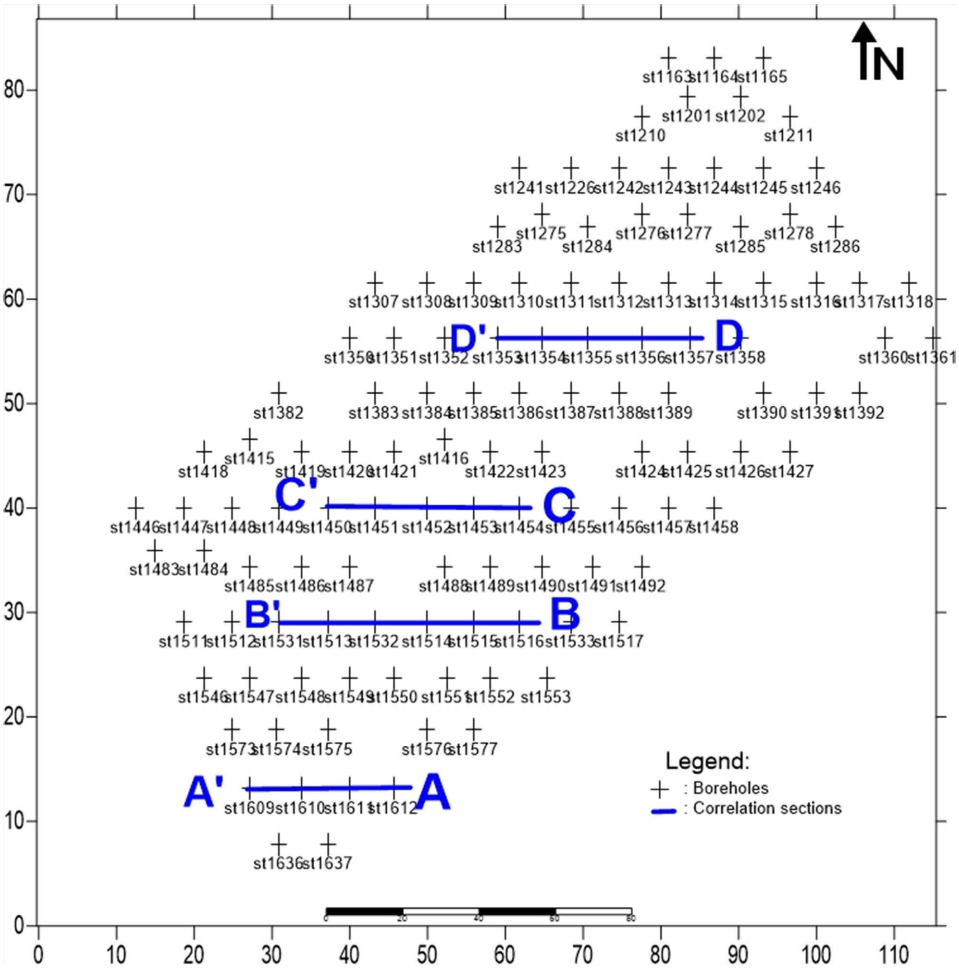

Figure 4. Map of the different lithostratigraphic sections.

vanadomolybdic reagent. The optical density of the yellow solution thus formed is measured with a spectrophotometer. The intensity obtained is a function of the mass concentration of content.

CaO

The sample is dissolved in perchloric acid. Calcium is chelated in the alkaline medium using excessive amounts of Ethylenediaminetetraacetic acid (EDTA). This excess is titrated with a calcium solution of known concentration, in the presence of magnesium to make the change more visible.

SiO_2

It is quantified by a dissolution of the sample by digestion with hydrofluoric acid, followed by a measurement of the silica content by atomic absorption spectrometer with a nitrogen oxide/acetylene flame at a wavelength of 251 nm.

The determination of these major elements allows the calculation of two exploitation parameters which are the carbonate parameter ($K = CaO/P_2O_5$) and the feral parameter ($\Phi = Al_2O_3 + Fe_2O_3$).

4. Results and Discussion

4.1. Correlation and Lithological Synthesis of the Different Sections

A'A section (Figure 5)

A'A section links four boreholes st1609, st1610, st1611, and st1612. Correlation established from these boreholes shows this succession from top to bottom:

More or less phosphatized sandstones that cover an average thickness of 1.7 m;

In the Silico-feralitic formation, crossed by boreholes st1612 and st1611, the so-called "off-layer" phosphate is found precisely at the level of the st1611 hole. The direct contact between this formation and the phosphate layer is due to the erosion of the roof clayey;

The Taiba formation is represented solely by heterogeneous phosphate with an average thickness of 4 m. A thickening between boreholes st1612 and st1610, and a thinning at borehole st1609 characterize it. The significant thickness noted in borehole st1610 is related to the presence of sand anomalies;

The Lam-Lam formation, made up of attapulgite-type laminated clay, has a thickness varying between 0.15 and 1.35 m the correlation shows that this irregular wall rises from east to west and then sinks at the level of borehole st1609.

B'B section (Figure 6)

B'B section connects five boreholes: st1515, st1514, st1532, st1513, and st1531. The correlation established from these boreholes is shown in figure X. The lithology comprises from top to bottom

The sandstone formation is crossed only by the borehole st1531 on a thickness of 0.8 m;

The Silico-feralitic formation is very represented in this section and is found in all the boreholes except in borehole st1513. Clay beds are encountered, also significant thicknesses of "off-layer phosphate" (3.7 m), notably in boreholes st515, st1532, and st1531. The formation has an average thickness of 2.53 m;

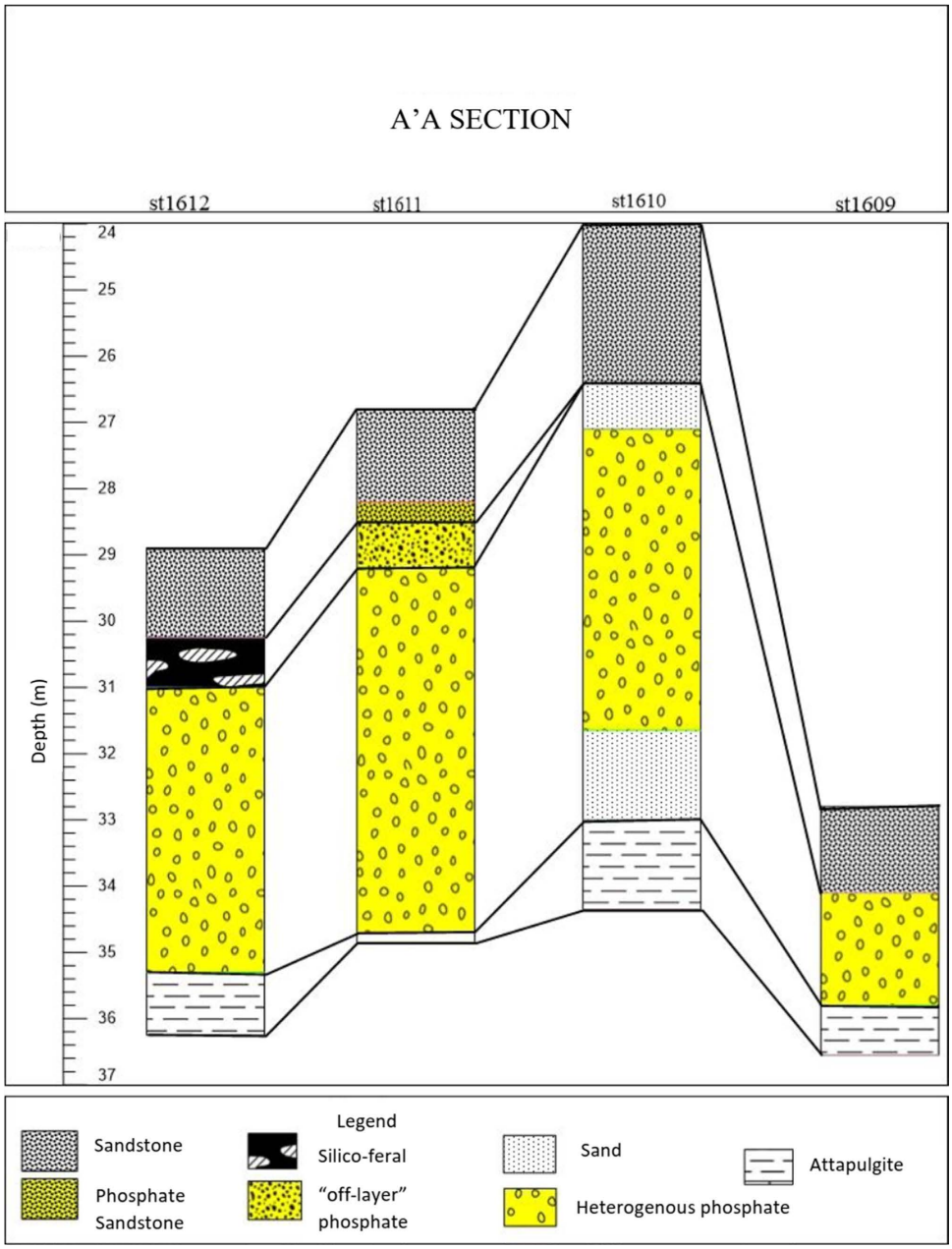

Figure 5. Correlation established from the A'A section.

The clayey roof is crossed only by the borehole st1531 on a thickness of 2 m;

The Taiba Formation comprises indurated phosphate in form of phosphate breccia with apatite pebbles, abundant flint phosphate, and homogeneous phosphate with intercalations of phosphate clay beds, and sand anomalies (st1515, st1532). The correlation also shows a thinning of the phosphate layer between boreholes st1515 and st1532 due to a rise of the wall thickness, then a thickening at the level of holes st1513 and st1531;

The wall (1.15 m thick), thins out until it disappears in borehole st1513 and then reappears in borehole st1531.

C'C section (**Figure 7**)

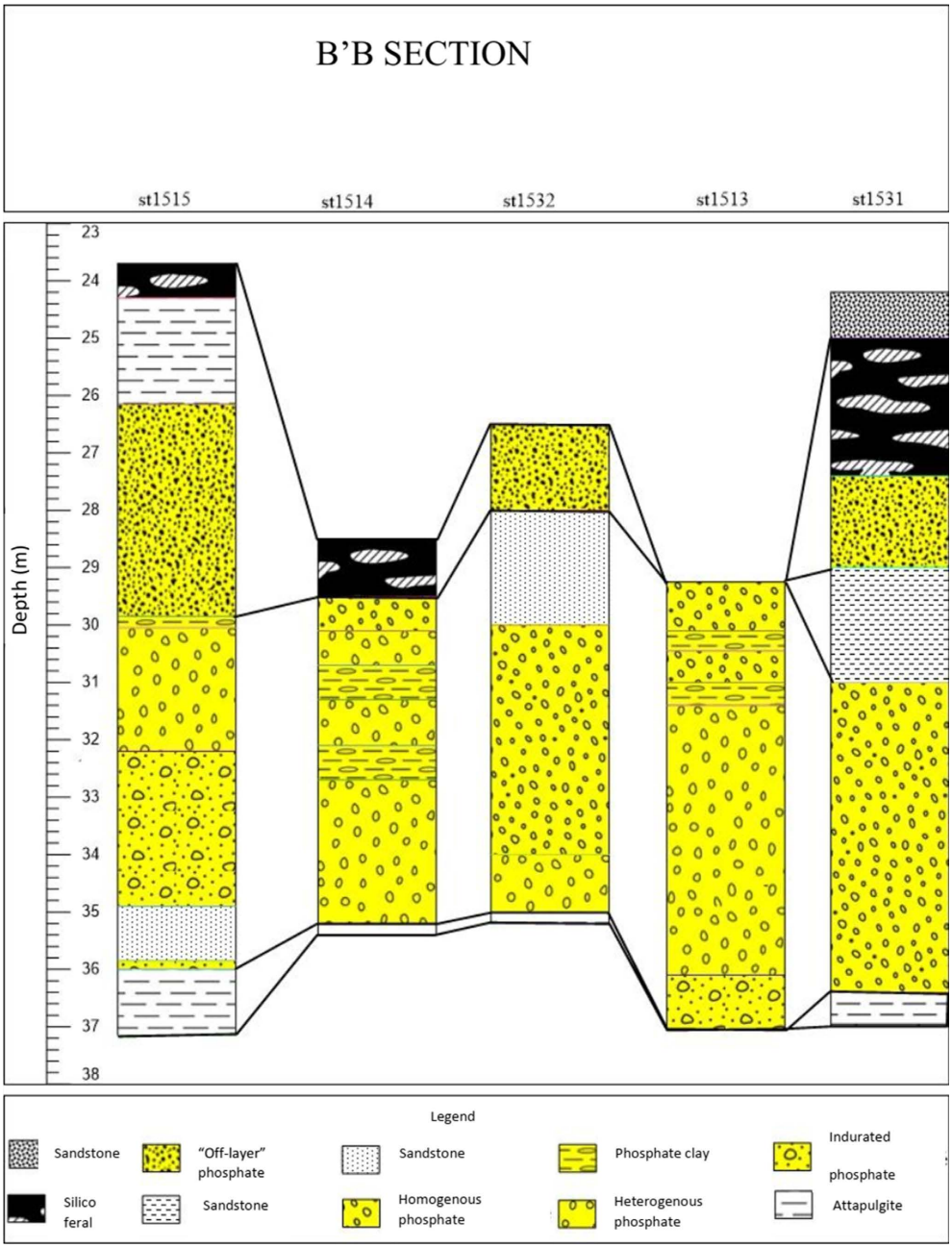

Figure 6. Correlation established from the B'B section.

C'C section links five boreholes, which are st1454, st1453, st1452, st1451, and st1450. Correlation established between the boreholes shows the following succession:

The sandstone formation present in borehole st1451 becomes armour-plated in borehole st1454. The average thickness of this formation is 2 m;

The silico-ferallitic formation is present in boreholes st1454, st1451, and st1450 with thicknesses up to 4.25 m. The formation contains beds of clay;

The clays of the roof present relatively low thicknesses, they are crossed by the boreholes st1454, st1452, and st1451 with an average thickness of 0.67 m;

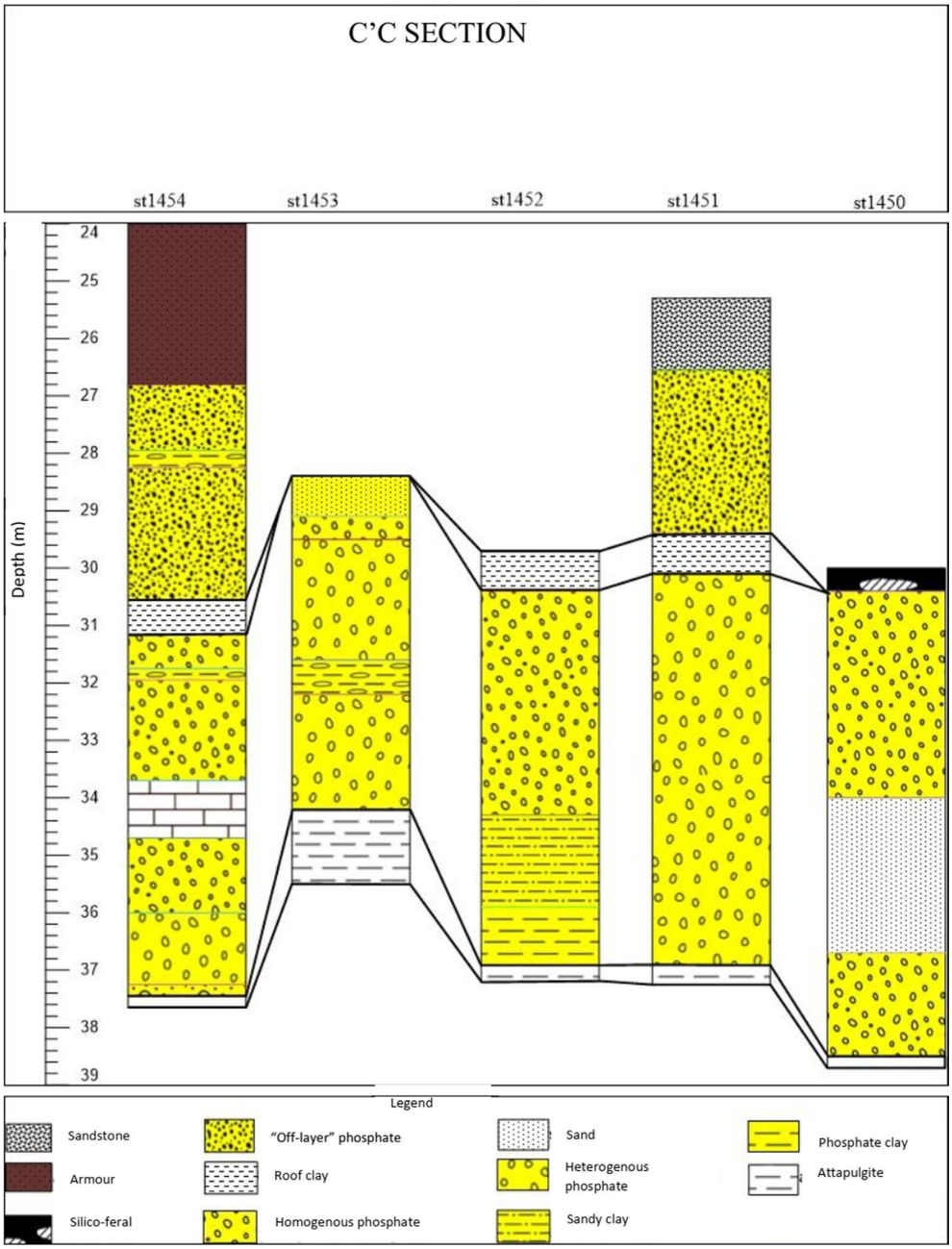

Figure 7. Correlation established from the C'C section.

The Taiba formation has an average thickness of 6.56 m. The correlation of the different boreholes established in this section shows that between boreholes st1450 and st1453, the phosphate layer becomes thinner with a rise in the thickness of the attapulgite wall and then thickens at the borehole st1454. The high thicknesses noted in this section are related to the presence of sand (st1450) and limestone (st1454) anomalies, but also the presence of sandy clay discordant to the Lam-lam formation (st1452);

The wall has a practically constant thickness but, at the level of the borehole st1453, we observe that this wall thickens and rises.

D'D section (Figure 8)

Section D'D connect five boreholes which are: st1357, st1356, st1355, st1354, and st1353. From top to bottom, these boreholes present the following succession:

The sandstone formation is crossed by the boreholes st1356 and st1353 with an average thickness of 3 m;

The silico-feralitic formation is very represented in this section, the "off-layer" phosphate which appears in the silico-feralitic formation can reach 3.7 m in thickness;

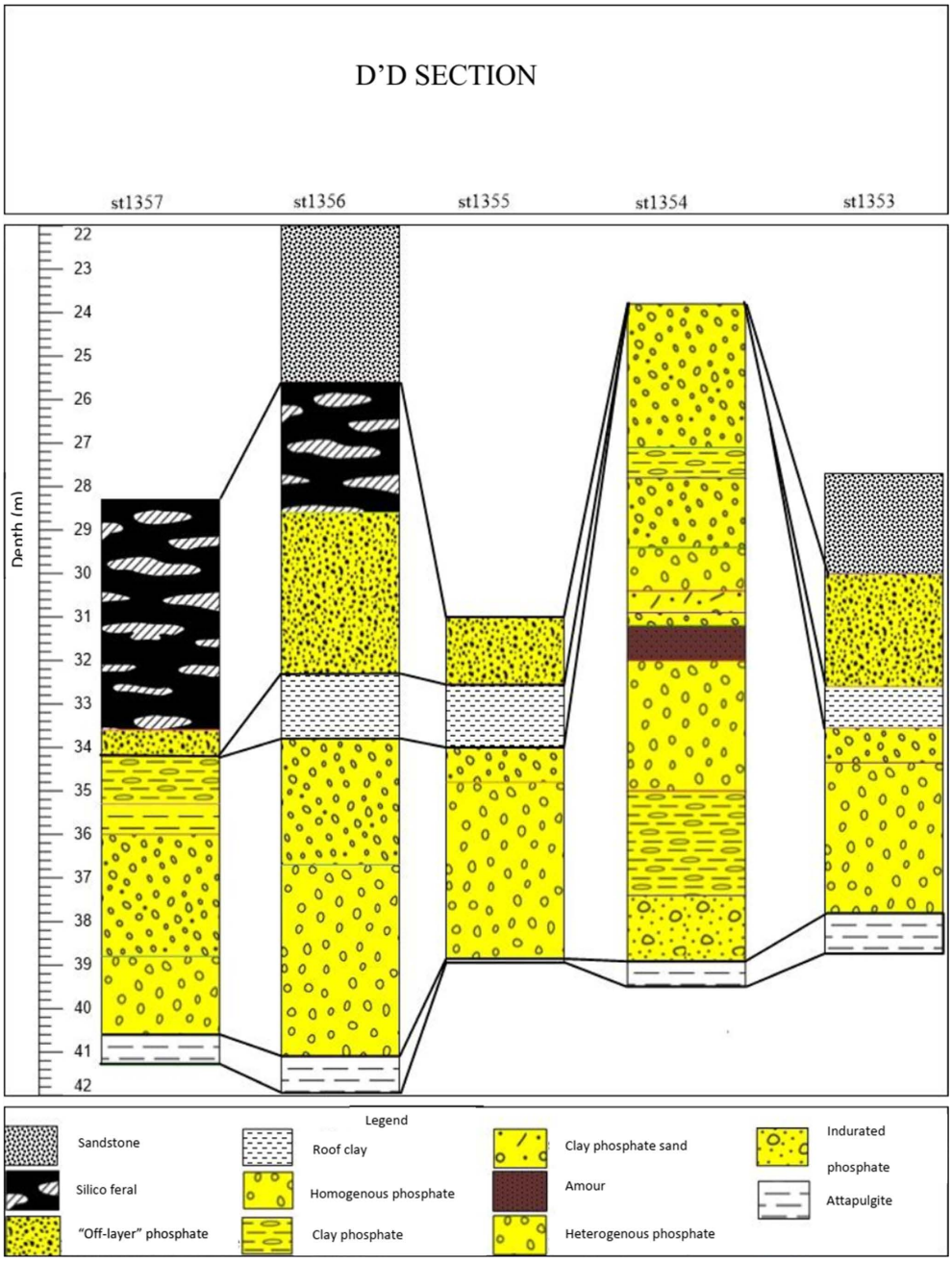

Figure 8. Correlation established from the D'D section.

The roof clays occur at nearly constant depths over an average thickness of 0.8 m. They are crossed by the boreholes st1356, st1355, and st1353;

The Taiba formation, which is very deep at the level of the borehole st1354, reaches a thickness of 11 m due to the presence of layer anomalies (armour, phosphate clay, clay-phosphate sand), on both sides of this borehole a thinning and a deepening of the phosphate layer is observed;

The wall shows a clear irregularity characterized by falling and rising.

The lithological succession described by [6] is not always verified in the Tobene Sud 1 area. The top of the phosphate layer is often eroded as well as the silico-feralitic formation. This erosion of the overlying layers can lead to direct contact between the sandstone formation and the Taiba Formation as mentioned by [7]. The silico-feralitic formation corresponds to lime phosphate altered to millisite and crandallite [7]. This alteration is mainly related to the absence of a protective layer (such as the roof clays) which is completely eroded exposing the ore to hot and humid climatic conditions [13]. The variation in thickness of the phosphate layer within the sector is confirmed by the study conducted by [2] who stated that the phosphate layer in Taiba is 5 to 12 m thick with an average of 7 m and precisely at Tobene the phosphate layer is 6 m thick. In addition [14] also highlighted some specific characteristics of the Tobene panel even though it presents the same lithological unit as the previously exploited panels. One of the characteristics is the lateral variations of the attapulgite wall which pass to limestone (confirmed in the borehole st1284).

4.2. Geochemical Analysis

4.2.1. Variation of Major Elements

P_2O_5

P_2O_5 percentage represents the content of phosphor in the ore. According to the algorithm of the "Normale Layer" implemented by the company, the percentage of P_2O_5 should be high than 20%. In the study area, the percentage of P_2O_5 is comprised between 17.85 and 36.32 and the average calculated based on the P_2O_5 percentage of each borehole is 31.4. The isocontents map of P_2O_5 (**Figure 9**) shows that the percentages comprise between 20% and 30% are more distributed in the sector. Moreover, an increase in this element is observed in the center and Nord-Est with percentages high than 32. The lowest values are found in the northwest as small enclaves. The best quality phosphate is therefore found in the center and northeast where the P_2O_5 content is higher than 32%.

SiO_2

It is present in boreholes with contents ranging from 6.06% to 56.05%. The silica distribution map (**Figure 10**) shows that low silica contents (<20%) are much more present in the center of the sector, and medium contents are confined to the North-East, and South-West and preferentially on the edges of the study area. The high contents found in boreholes st1382, st1383, st1354, st1573, st1490, st1446, st1226, and st1354 are due to the presence of pockets of sand or flint in the phosphate layer. According to (repartition des oxides de phosphates), the

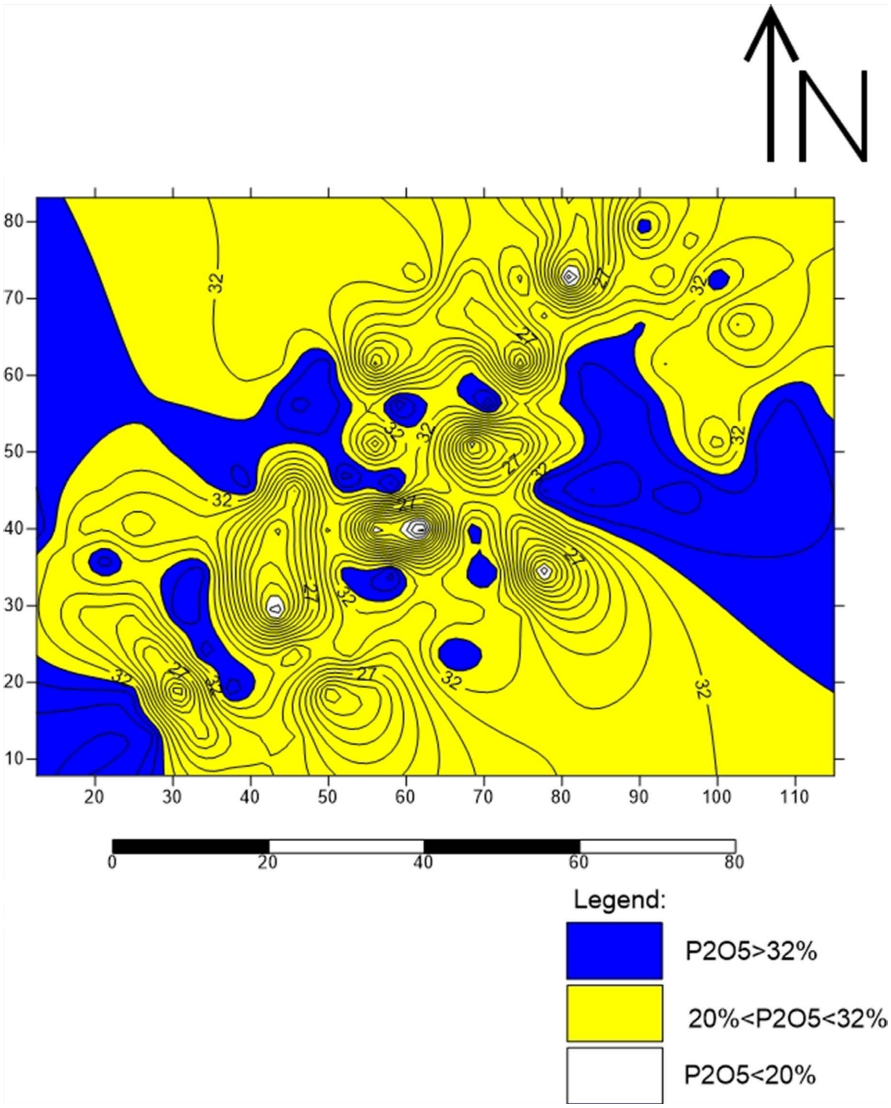

Figure 9. Isocontent map of P_2O_5.

presence of the silica inside the phosphate layer is related to the irregular structure of the latter, marked by collapses which are seats for the accumulation of sands.

Feral

The feral defined by $\Phi = Fe_2O_3 + Al_2O_3$ is mainly found at the top and inside of the phosphate layer [15] (Samb, 2007). It has a negative influence on production because at the level of chemistry, it is an additional element in the phosphoric acid and its presence in the ore makes selection difficult. The reference value set by the "Industrie Chimique du Senegal" is 3%. Chemical analysis of the boreholes samples in the area reveals that the feral varies between 0.58% and 19.30%. The feral isocotents map (Figure 11) shows that the center of the sector is dominated by contents less than 3%, whereas medium and high contents are present in forms of enclaves in the North-East and South-West. According to [15] (Samb, 2007), the development of the feral in the Eastern, South-Western, and South-Eastern parts of the Tobene sector is favored by the structure of the

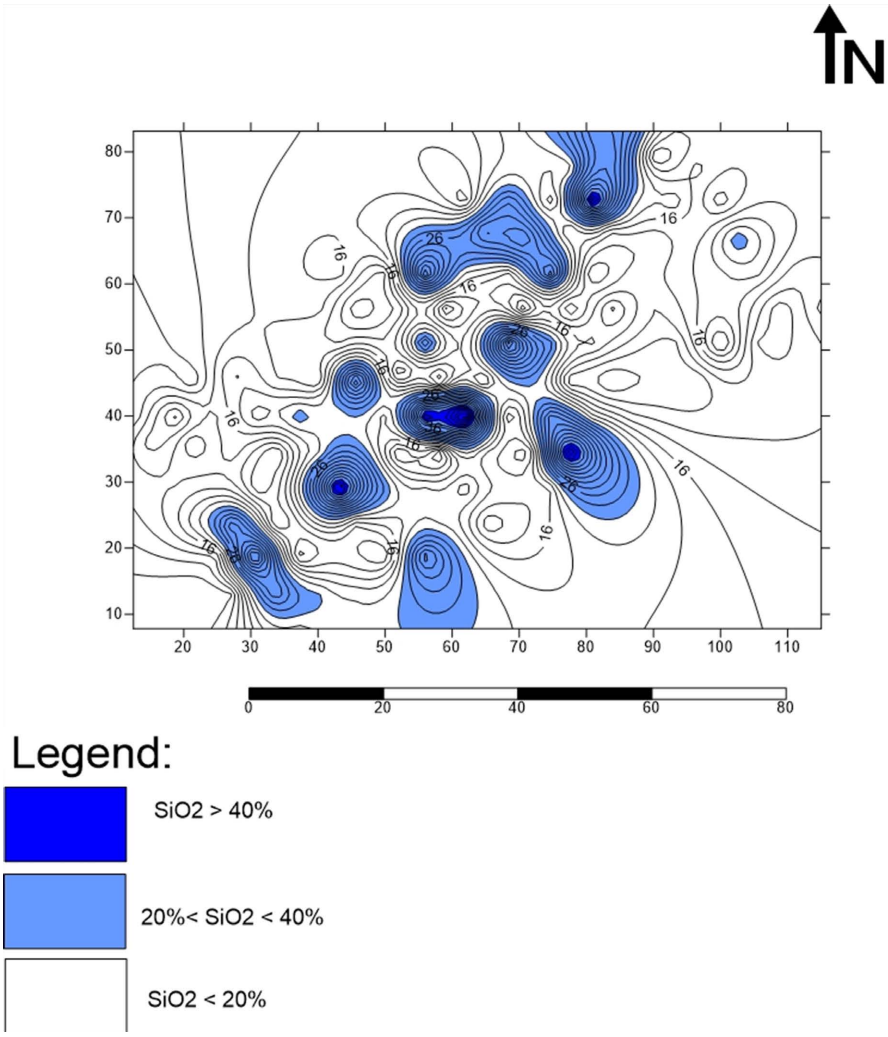

Figure 10. Isocontent map of the Slica.

deposit and the wavy morphology of the roof and wall of the phosphate layer.

Distribution of the K value (CaO/P_2O_5 ratio)

The K value represents the ratio CaO/P_2O_5; it varies between 0.9 and 2.1 in the sector. In Taiba the K value is 1.45. For K values > 1.45, the ore is carbonated. The k variability map (Figure 12) indicates an average K value in the sector equal to 1.3 but it exceeds 1.57 in the North, forming an enclave that indicates the presence of carbonate ore. Boreholes st1286, st1285, and st1284 reveal the presence of limestone layers interspersed in the phosphate layer but also at the base of the layer. The presence of limestone in the North East sector of the Taiba deposit has been described by [10] [16] (Atger, 1970; Brancart and Flicoteaux, 1971), indeed in Tobene as well, few limestones are found within the phospharenite layer.

4.2.2. Correlation between Major Elements

Correlation between P_2O_5 and CaO

Many sedimentary phosphates are mineralogically composed of Fluor-apatite carbonate of the formula $Ca_{10}(PO_4, CO_3)_6F_{2\text{-}3}$. The correlation test using RStudio

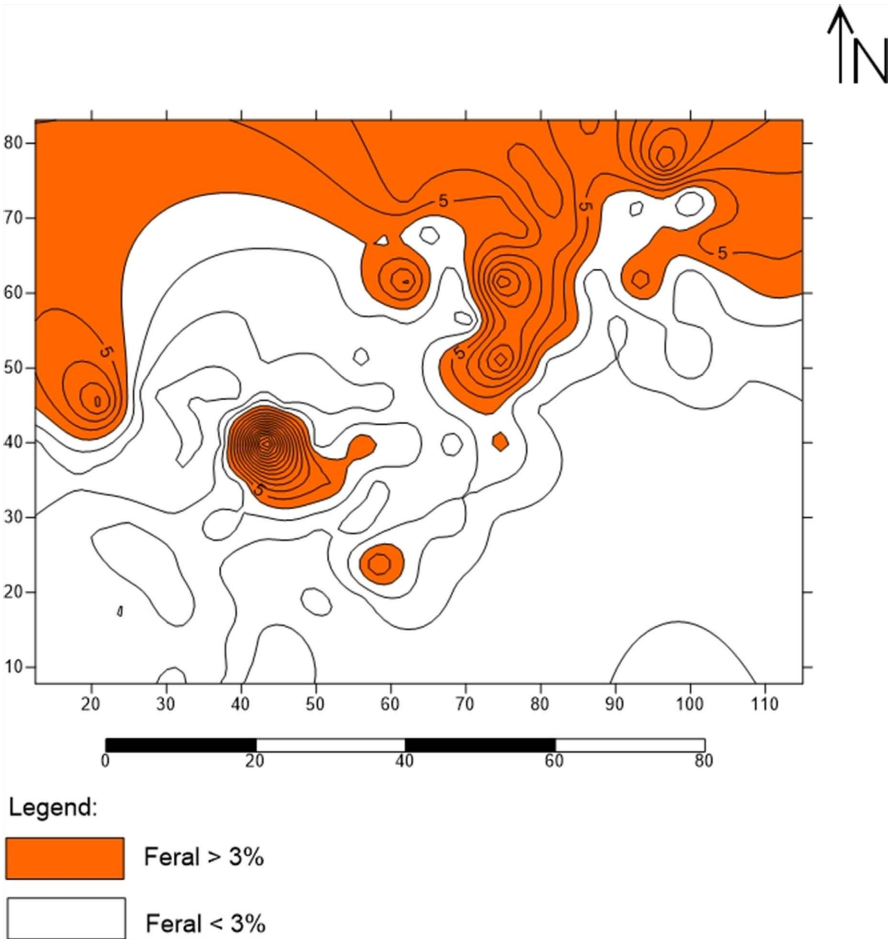

Figure 11. Isocontents map of feral.

shows that:

$$t = 24.396,\ df = 119,\ p\text{-value} < 2.2e{-}16$$

Alternative hypothesis: true correlation is not equal to zero, 95 percent confidence interval: 0.8773576 0.9384661

p-value <<< 0.05 we reject the Null Hypothesis which means there is a strong relationship between P_2O_5 and CaO. The assumption is confirmed by Figure 13, which shows that the distribution of the scatterplots is preferentially along the regression line.

Sample estimates: Pearson's correlation coefficient = 0.9128906 shows that the contents of P_2O_5 and CaO vary in the same direction; an increase in P_2O_5 is accompanied by an increase in CaO.

Correlation between P_2O_5-SiO_2

A result from the correlation test shows that

$$t = -25.264,\ df = 119,\ p\text{-value} < 2.2e{-}16$$

95 percent confidence interval: −0.9421743 −0.8845288

sample estimates Pearson's correlation: −0.9180748

Alternative hypothesis: true correlation is not equal to zero

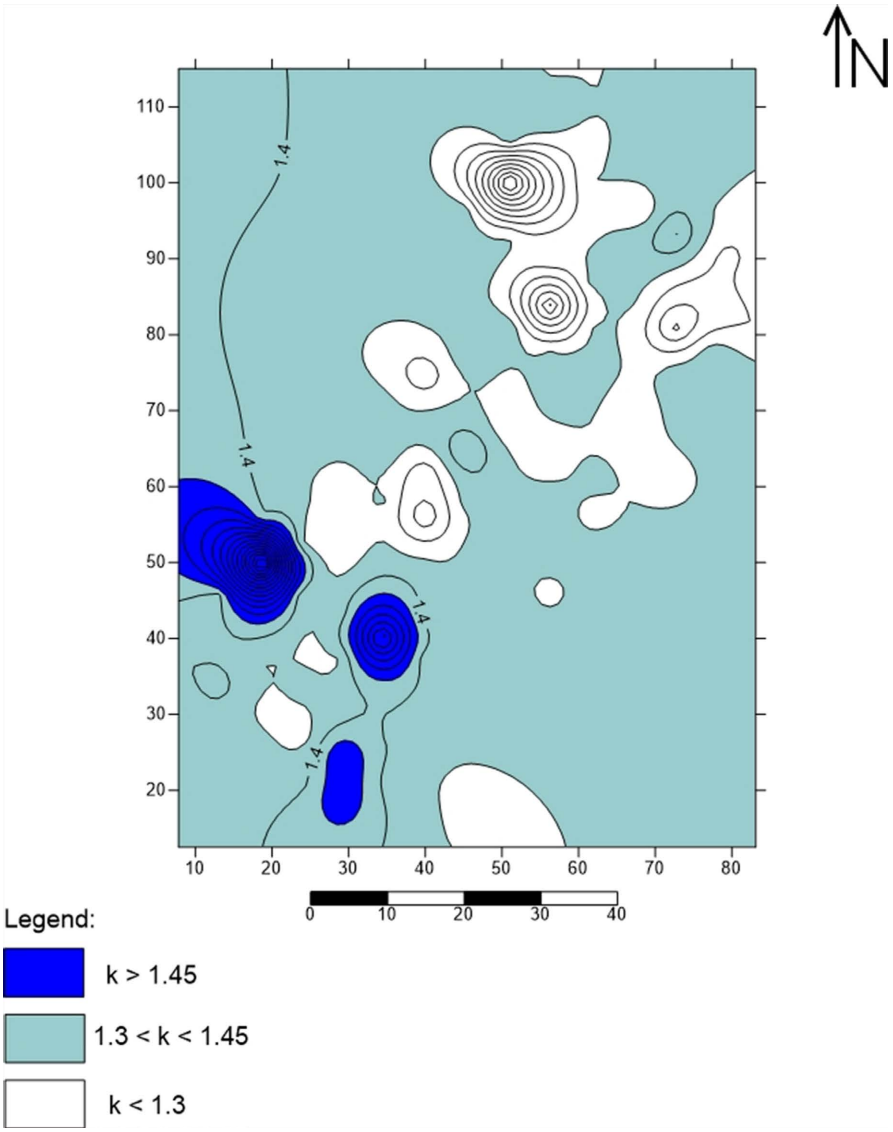

Figure 12. Variability map of the K value ($CaOP_2O_5$).

The analysis of the diagram in (Figure 14) shows a slight dispersion of the P_2O_5 and SiO_2 variables and the negative value of Pearson's correlation coefficient of the regression line (−0.9180748 indicates an evolution in the opposite direction. A high P_2O_5 content is correlated with a low SiO_2 percentage nevertheless the p-value <<< 0.05, the null hypothesis is rejected

Correlation between P_2O_5 and Feral

The relationship between P_2O_5 and feral allows assessment of the quality of the ore. The manufacture of phosphoric acid requires an ore with a feral content of less than 3%. Results from the statistical correlation show:

t = −4.7319, df = 119, p-value = 6.18e−06

Alternative hypothesis: true correlation is not equal to zero
95 percent confidence interval: −0.5382149 −0.2362329
sample estimates Pearson's correlation = −0.3979492

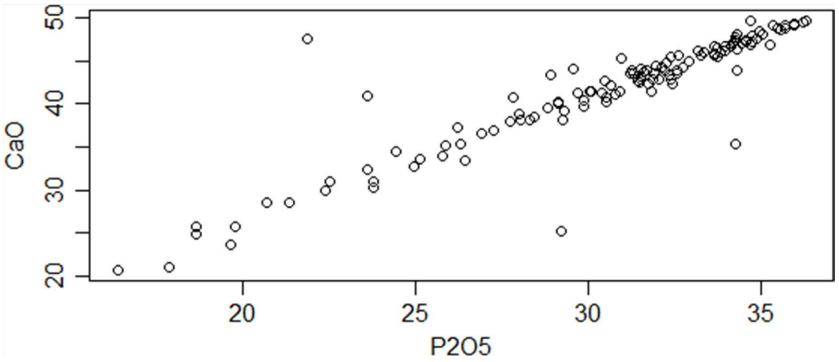

Figure 13. Correlation between CaO and P_2O_5.

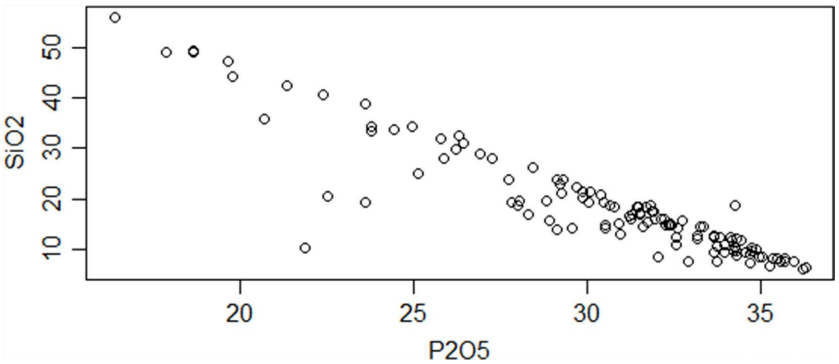

Figure 14. Correlation between SiO_2 and P_2O_5.

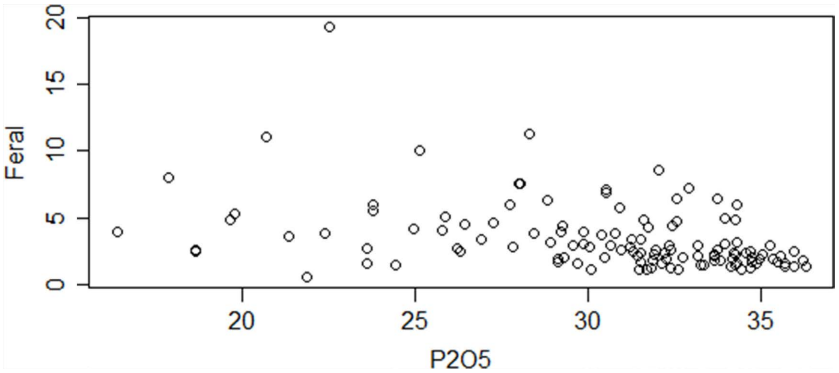

Figure 15. Correlation between Feral and P_2O_5.

The correlation diagram in Figure 15 shows a strong dispersion of scatter-plots on both sides of the regression line; on the other hand, the negative value of Pearson's correlation (−0.3979492) of this line defines an evolution of the mineral (Fe_2O_3 + Al_2O_3) and P_2O_5 parameters in the opposite direction.

5. Conclusion

Covered by a set of 117 boreholes, the Tobène SUD1 sector is characterized from top to bottom by the lithostratigraphic succession: the sandy overburden, the sandstone formation, the Silico-feralitic formation, the variegated roof clays, the Taiba formation (homogeneous ore and heterogeneous ore), and the foliated attapulgite of the wall. In the study area the phosphate layer, whose thickness does

not exceed 11.2 m, is overlain by the clays roof, which is eroded in many boreholes. A rise in the clay wall, which in some boreholes changes to limestone, is also noted in the area. In Tobène South 1 area, a significant presence of the "off-layer phosphate" often discordant to the ore, as well as sand layer anomalies at different levels within the phosphate layer is noticed. Results from the geochemical analysis have allowed us to generate isocontent maps and study the distribution of the five major oxides in the area. The average concentration of P_2O_5 is 31.43%; however, the area is dominated by concentrations between 20% and 32%. The importance of the feral content accentuated by the erosion of the clay roof is one of the characteristics of the sector. Indeed the average content of feral is 3.33%. Silica is unequally distributed in the sector; its average concentration is estimated at 17.9%. The correlation diagrams show on one hand a proportionality in the evolutions between the chemical variables CaO and P_2O_5, on the other hand, an opposite evolution between P_2O_5 and the two chemical parameters silica (SiO_2) and feral.

Acknowledgments

The author is grateful to Industries Chimiques du Sénégal (ICS) for the availability of the data, to my supervisor Professor Mouhamadoul Bachir Diouf, and the lecturers of the Geology Department of the Faculty of Sciences and Technologies, Cheikh Anta Diop University of Dakar.

Conflicts of Interest

The authors declare no conflicts of interest regarding the publication of this paper.

References

[1] Ndiaye, M., Ngom, P.M., Gorin, G., Villeneuve, M., Sartori, M. and Medou, J. (2016) A New Interpretation of the Deep-Part of Senegal-Mauritanian Basin in the Diourbel-Thies Area by Integrating Seismic, Magnetic, Gravimetric and Borehole Data: Implication for Petroleum Exploration. *Journal of African Earth Sciences*, **121**, 330-341. https://doi.org/10.1016/j.jafrearsci.2016.06.002

[2] Prian, J.-P. (2014) Phosphate Deposits of the Senegal-Mauritania-Guinea Basin (West Africa): A Review. *Procedia Engineering*, **83**, 27-36. https://doi.org/10.1016/j.proeng.2014.09.008

[3] Barusseau, J.P., Duvail, C., Noël, B.J., Nehlig, P., Roger, J. and Serrano, O. (2009) Notice explicative de la carte géologique du Sénégal à 1/500 000, feuilles nord-ouest, nord-est et sud-ouest. 62.

[4] Wu, Y., Wang, J., Wang, Q., Li, H., Zhang, N. and Xiao, Y. (2019) Geochemical Features and Genetic Mechanism of Deep-Water Source Rocks in the Senegal Basin, West Africa. *Thermal Science*, **23**, 2641-2649. https://doi.org/10.2298/TSCI181130153W

[5] Villeneuve, M., Fournier, F., Cirilli, S., Spina, A., Ndiaye, M., Zamba, J., Viseur, S., Borgomano, J. and Ngom, P.M. (2015) Structure of the Paleozoic Basement in the Senegalo-Mauritanian Basin (West Africa). *Bulletin de La Société Géologique de France*, **186**, 193-203. https://doi.org/10.2113/gssgfbull.186.2-3.193

[6] Samb, E.M. (1993) Etude géologique et estimation des réserves du panneau de Tobène. Rapport interne CSPT, 65 p.

[7] Lucas, J., Menor, E. and Prévôt, L. (1979) Le gisement de phosphate de chaux de Taïba (Sénégal) Un exemple d'enrichissement par altération. *Sciences Géologiques. Bulletin*, **32**, 39-57. https://doi.org/10.3406/sgeol.1979.1554

[8] Brownfield, M.E. (2016) Assessment of Undiscovered Hydrocarbon Resources of Sub-Saharan Africa. USGS Numbered Series No. 69-GG; Data Series, Vols. 69-GG. U.S. Geological Survey. https://doi.org/10.3133/ds69GG

[9] Samb, M. (2008) Géologie, Minéralogie, Pétrographie et Géochimie Minérale des Phosphates Sédimentaires du Gisement de Tobène (Sénégal) Application à une Exploitation Industrielle. Thèse de Doctorat d'Etat, U.C.A.D., I.S.T., Sénégal.

[10] Brancart, R. and Flicoteaux, R. (1971) Age des formations phosphatées de Lam-Lam et Taïba (Sénégal Occidentale) Données micropaléontologiques, conséquences stratigraphiques et paléogéographiques. *Bulletin de la Société géologique de France*, **13**, 399-408. https://doi.org/10.2113/gssgfbull.S7-XIII.3-4.399

[11] Tessier, F. (1952) Contributions à la stratigraphie et à la paléontologie de la partie ouest du Sénégal. Thèse Univ. Marseille, et. Dir. Mines Géol. Afr. occ. fr, 14 (1952), 2 t., 544 p.

[12] Flicoteaux, R. and Tessier, F. (1971) Précisions nouvelles sur la stratigraphie des formations du plateau de Thiès (Sénégal occidental) et sur leurs altérations. Conséquences paléogéographiques. *Comptes Rendus de l'Académie des Sciences, Paris*, **272**, 364.

[13] Moustapha, D., Mamadou, F., Mouhamadou, B.D., *et al.* (2016) Mineralogical Characterization of the Sedimentary Phosphate Deposit of Tobène (Western Senegal). *Journal of Shipping and Ocean Engineering*, **6**, 226-240. https://doi.org/10.17265/2159-5879/2016.04.005

[14] Dione, N.P., Diagne, M., Diouf, M.B., Fall, M. and Giresse, P. (2018) Petrography and Mineralogy of the Eocene Phosphate Deposit of Tobène (Taïba, Senegal). *Journal of Geoscience and Environment Protection*, **6**, 193-209. https://doi.org/10.4236/gep.2018.65016

[15] Samb, M. (2007) Repartition des facies phosphates oxydes dans le gisement de Tobene (Sénégal): Guide d'exploitation.

[16] Atger, M. (1970) Données sur la géologie du gisement de phosphate de Taïba et les gisements d'origine sédimentaire marine. Rap. Int. Inédit 70-AT-06, Comp. Sénég. Phosph. Taïba, Serv. Géol. Prospect., 14 p.